Electrochemiluminescence Devices Consisting of ZnO Nanorods Vertically Grown on Substrate

Tomohito Tanaka,[1] Hiroshi Takishita,[1] Takashi Sagawa,[2] Susumu Yoshikawa,[2] and Shuzi Hayase*[1]
[1]*Kyushu Institute of Technology, 2-4 Hibikino, Wakamatsu-ku, Kitakyushu 808-0196*
[2]*Institute of Advanced Energy, Kyoto University, Gokasho, Uji, Kyoto 611-0011*

(Received April 1, 2009; CL-090323; E-mail: hayase@life.kyutech.ac.jp)

Unique behaviors of electrochemiluminescence from a device consisting of ZnO nanorod (Cell-1) are reported. Cell-1 emitted more intense electrochemiluminescence than cell consisting of two flat electrodes (Cell-2). The onset potential at which the emission starts was 1.5 V for Cell-1, which was lower than 2.5 V for Cell-2. The unique behaviors were explained by asymmetric collision modes of emitting species (Ru^{I} and Ru^{III}) in the nanospace among ZnO nanorods and were characteristic to the ZnO nanorod array.

Electrochemiluminescence (ECL) originates from solutions consisting of emitting molecules.[1] For example, ECL from Ru complexes, Ir complexes, rubrene, poly(phenylenevinylene), and PBDOHF (poly[9,9-bis(3,6-dioxaheptyl)fluorine-2,7-diyl]) has been reported.[2] Among them, ECL from tris(bipyridyl)ruthenium salts [$Ru(bpy)_3^{2+}$] has been intensively studied.[2] Recently, we have reported that an intense electroluminescence was observed from nanospace of titania nanohole arrays.[3–5] We concluded that the high intensity emission is caused by the increase in the amount of electrons injected from the TiO_2 nanohole arrays with large surface areas and the increase in the collision frequency between these emitting species (Ru^{I} and Ru^{III}) in the restricted nanospace of the nanohole arrays. In the meantime, it has been reported that ZnO nanorods grow vertically on a flat substrate.[6] This prompted us to use the ZnO nanorods as an electrode for the ECL device.

$Ru(bpy)_3(PF_6)_2$ abbreviated to Rubpy was used for the emitting species.[7] ZnO nanorod arrays were prepared as follows,[6,8] 0.01 M zinc acetate solution in ethanol was spin-coated onto a FTO substrate. The substrate was baked at 130 °C for 1 h, 180 °C for 1 h, and 260 °C for 2 h. The substrate was then dipped in a mixture of 0.8 M aqueous NaOH and 0.04 M zinc nitrate solution. The container was heated at 110 °C for 4 h. In order to obtain thick ZnO layers, the treatment by zinc nitrate was carried out repeatedly.

Cell-1 has the following configuration: Glass/F-doped SnO_2 (FTO, 30 Ω/square, Nippon Sheet Glass)/ZnO nanorod/emitting layer consisting of Rubpy in propylene carbonate/FTO glass (Figure 1). Cell-2 (a reference cell) consists of FTO glass/Rubpy in propylene carbonate/FTO glass. Cell-1 was prepared as follows: A spacer polymer (Himilan, DuPont Mitsui Polychemicals, thickness 50 μm) was sandwiched between a FTO grass with ZnO nanorods and a FTO glass (a counter electrode). Rubpy solution in propylene carbonate was injected into the space of the two electrodes. The cell was encapsulated with a room-temperature cure-type epoxy resin (Araldite standard 30122 and 30123, Vantico). The emitting area was 10 × 10 mm^2. An AFG310 (Tektronix) function generator was used to apply AC rectangular wave potentials to the ECL cell. The

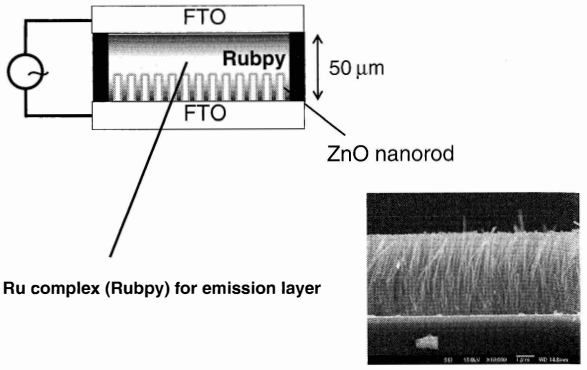

Figure 1. ECL device structure consisting of ZnO nanorods (Cell-1).

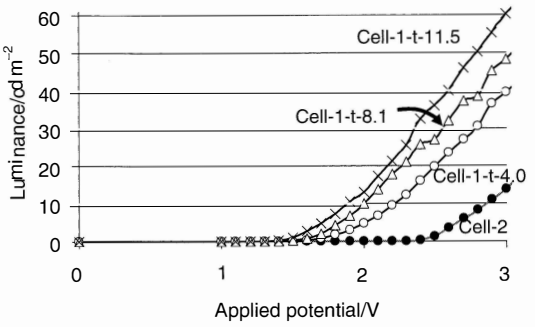

Figure 2. Relationship between luminescence and applied potential (AC 60 Hz). Cell-1-*X*: *X* stands for the length of ZnO nanorods.

ECL response was observed with a Topcon Model BM-9 luminance meter.

ECL intensity for Cell-1 was higher than that of Cell-2 as shown in Figure 2. The onset potential at which the emission starts was 1.5 V for Cell-1, which was lower than 2.5 V for Cell-2. In addition, the onset potential decreased as the ZnO nanorods became thicker. The results strongly demonstrate that the decrease in the onset potential is associated with the ZnO nanorod structure.

The current–potential curve showed that the current density of Cell-1 was higher than that of Cell-2 at each potential. In addition, the current density increased with an increase in the ZnO-nanorod thickness. For example, the current density was 29 mA cm^{-2} for Cell-2, 46 mA cm^{-2} for Cell-1-t-4.0 (length of ZnO nanorod: 4.0 μm), 50 mA cm^{-2} for Cell-1-t-8.1 (length of ZnO nanorod: 8.1 μm), and 52 mA cm^{-2} for Cell-1-t-11.5 (length of ZnO nanorod: 11.5 μm) at 3 V, where *X* of Cell-1-t-*X* stands for the length of the ZnO nanorod. The large surface area of the ZnO nanorods would be responsible for the higher

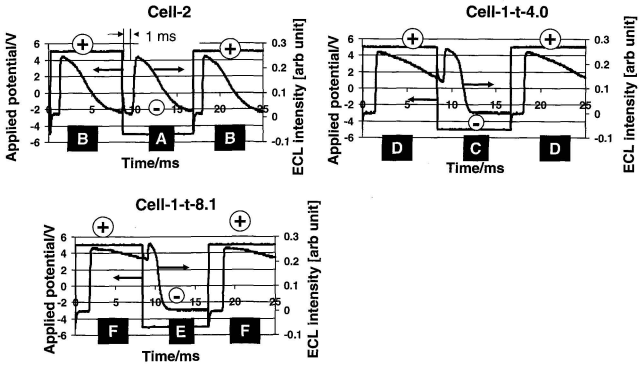

Figure 3. Response curve of ECL. Applied potential: Potential applied to an electrode with ZnO nanorods.

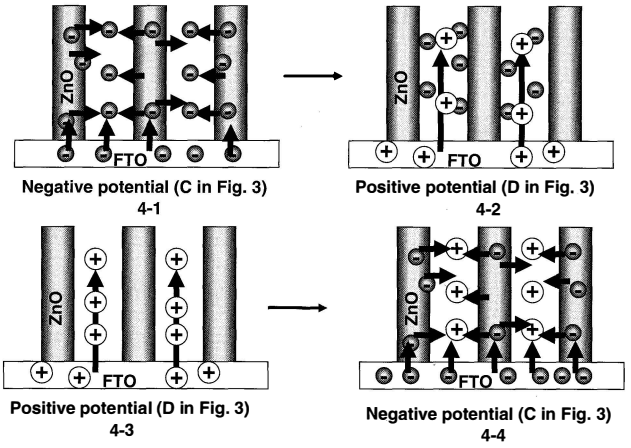

Figure 4. Proposed mechanisms for asymmetric response curves. ⊖: Ru^{I}, ⊕: Ru^{III}.

current density, because they are an n-type semiconductor and electrons can diffuse in the ZnO nanorods. The ECL efficiency of Cell-1 was higher than that of Cell-2, and the efficiency increased as the ZnO nanorods became thicker. For example, the efficiency was 0 lm W^{-1} for Cell-2, 0.03 lm W^{-1} for Cell-1-t-4.0, 0.07 lm W^{-1} for Cell-1-t-8.1, and 0.10 lm W^{-1} for Cell-1-t-11.5. The high efficiency of Cell-1-t-11.5 can be explained by the increase in the collision frequency between these emitting species (Ru^{I} and Ru^{III}) not by mere increase in the amount of electrons injected from the vast surface of the ZnO nanorods.

Figure 3 shows the time-dependent response of ECL for Cell-1-t-4.0, Cell-1-t-8.1, and Cell-2, where polarity of the potential is described as that of an electrode with ZnO nanorods. The response curve of Cell-2 on polarity change from positive to negative (A region in Figure 3) was the same as that from negative to positive (B region in Figure 3) because the cell structure is symmetrical. However, the response curve for Cell-1-t-4.0 had a sharp peak on the polarity change from positive to negative (C region in Figure 3), and a broad peak on the polarity change from negative to positive (D region in Figure 3). In the case of Cell-1-t-8.1 which has a thicker ZnO nanorod layer than Cell-1-t-4.0, the difference in the response curve between E and F regions (Figure 3) was pronounced more than that between C and D regions; namely, the slop of the curve in F region was gentler than that in D region. The asymmetrical response curve can be explained by a model shown in Figure 4. ECL originates from Ru^{II*} which is formed by the collision of Ru^{I} and Ru^{III}, where the former is formed on a cathode and the latter is formed on an anode. In the case of Cell-1, Ru^{II} was reduced to Ru^{I} on the surface of both a transparent conductive layer (F-doped SnO_2, FTO) and ZnO nanorods when the negative potential was applied (Figure 4-1), during which the nanospace among ZnO nanorods is filled with Ru^{I} (Figure 4-1). After the polarity was changed from negative to positive, Ru^{II} was oxidized to Ru^{III} on the surface of the FTO only not on the surface of ZnO nanorods (Figure 4-2), because ZnO has n-type character. The Ru^{III} gradually diffuses in the nanospaces among the ZnO nanorods and collides with Ru^{I} remaining in the nanospaces. Therefore, the emission lasts for a long time. The response curve of C region is explained as follows: When the positive potential is applied, Ru^{III} diffuses from the bottom of the FTO surface not from the surface of the ZnO nanorods. The nanospace is filled with Ru^{III} (Figure 4-3). When the polarity was changed from positive to negative, electrons are injected from both of the ZnO nanorod and FTO surfaces to form Ru^{I} (Figure 4-4). Therefore, Ru^{III} is surrounded immediately by Ru^{I}, and the collision between Ru^{I} and Ru^{III} occurs swiftly, resulting in giving a sharp emission curve (C in Figure 3). The difference in the response curves between E and F regions was much more pronounced because Cell-1-t-8.1 has thicker ZnO nanorods. The broad emission of D and F regions is responsible for the increase in the emission strength. Results of Cole–Cole plot supported the explanation that the diffusion of Ru ion species is supressed in Cell-1. For example, a semicircle associated with Ru ion diffusion is about 80 Ω for Cell-1 and 40 Ω for Cell-2. The interaction between Ru ion and ZnO nanorod surface may be responsible for the slow diffusion. Results on CV measurements of Cell-1 showed that the reduction potential of Ru^{II} shifted positively by 1.0 V, compared with that of Cell-2. The difference between the onset potentials for reduction and oxidation of Ru^{II} observed by the CV measurements was 2.5 V for Cell-2, and 1.5 V for Cell-1. These values are consistent with 2.5 V of onset potentials at which emission starts for Cell-2 and 1.5 V for Cell-1. In this stage, the reason why the reduction potential and the onset potential for emission of Cell-1 were extensively lower than that of Cell-2 is not fully understood.

References

1 P. McCord, A. J. Bard, *J. Electroanal. Chem.* **1991**, *318*, 91.
2 M. M. Richter, *Chem. Rev.* **2004**, *104*, 3003.
3 S. Okamoto, K. Soeda, T. Iyoda, T. Kato, T. Kado, S. Hayase, *J. Electrochem. Soc.* **2005**, *152*, A1677.
4 T. Kado, M. Takenouchi, S. Okamoto, W. Takashima, K. Kaneto, S. Hayase, *Jpn. J. Appl. Phys.* **2005**, *44*, 8161.
5 K. Ide, M. Fujimoto, T. Kado, S. Hayase, *J. Electrochem. Soc.* **2008**, *155*, B645.
6 M. Law, L. E. Greene, J. C. Johnson, R. Saykally, P. Yang, *Nat. Mater.* **2005**, *4*, 455.
7 J. N. Braddock, T. J. Meyer, *J. Am. Chem. Soc.* **1973**, *95*, 3158.
8 S. Yoshikawa, J. Aranami, PCT Int. Appl. WO2006129650.

Published on the web (Advance View) July 5, 2009; doi:10.1246/cl.2009.742